

RESOURCE-EFFICIENT SEPARATION TRANSFORMER

Luca Della Libera^{*1}, Cem Subakan^{*2,1,3}, Mirco Ravanelli^{1,3},
Samuele Cornell⁴, Frédéric Lepoutre⁵, François Grondin⁶

¹Concordia University, ²Université Laval, ³Mila-Quebec AI Institute,
⁴Università Politecnica delle Marche, ⁵Soundskrit Inc., ⁶Université de Sherbrooke

ABSTRACT

Transformers have recently achieved state-of-the-art performance in speech separation. These models, however, are computationally demanding and require a lot of learnable parameters. This paper explores Transformer-based speech separation with a reduced computational cost. Our main contribution is the development of the Resource-Efficient Separation Transformer (RE-SepFormer), a self-attention-based architecture that reduces the computational burden in two ways. First, it uses non-overlapping blocks in the latent space. Second, it operates on compact latent summaries calculated from each chunk. The RE-SepFormer reaches a competitive performance on the popular WSJ0-2Mix and WHAM! datasets in both causal and non-causal settings. Remarkably, it scales significantly better than the previous Transformer-based architectures in terms of memory and inference time, making it more suitable for processing long mixtures.

Index Terms— Efficient speech separation, Transformer, self-attention, deep learning.

1. INTRODUCTION

In recent years, deep learning has become more and more computationally demanding. The current trend consists of improving the performance of Deep Neural Networks (DNNs) through ever-larger models crunching ever-larger amounts of data. In natural language processing (NLP), this tendency led to large language models such as GPT3 [1], PaLM [2], Megatron [3] and many others. Similarly, large neural networks like wav2vec2.0 [4] and HuBERT [5] have gained popularity for speech processing. Large neural models, however, are energy-demanding, causing high inference costs (with considerable CO2 emissions [6]) that limit their widespread adoption in production systems. Moreover, such models cannot process users' data on the device, thus raising privacy concerns [7]. Efficient deep learning has been the object of recent research efforts. Approaches such as distillation [8], neural network pruning [9, 10], and binarization/quantization [11, 12] have been explored. In the context of speech processing, various efficient methods for speech enhancement/separation [13–19], keyword spotting, language identification [20], emotion recognition [21], and automatic speech recognition [22] have been proposed.

Among all the popular neural models, Transformers [23] are particularly difficult to make computationally efficient due to their quadratic memory bottleneck and the high number of parameters that they typically require. Revised Transformer-based architectures, which relax the quadratic memory requirement, [24] such as the Linformer [25], Longformer [26], and Reformer [27] have been proposed recently. Efficient Transformers have been studied for speech processing tasks as well, such as speech recognition [28], enhancement,

and separation [18]. These previous works, however, do not consider causal models suitable for on-device real-time applications.

In this paper, we propose a novel small-footprint speech separation model built upon the SkiM framework [19], called Resource-Efficient Separation Transformer (*RE-SepFormer*), that represents a lightweight alternative to the recently-proposed SepFormer. Unlike the SepFormer, the RE-SepFormer uses non-overlapping chunks in the latent space and, therefore, it reduces by half the number of chunks to process (if we consider the default overlap rate of 50%). Moreover, we further reduce the computations by using a special mechanism called *Memory Transformer*. The Memory Transformer operates over a summary representation calculated from whole chunks rather than attending every single element of the chunk independently.

We conducted the experimental validation on the popular WSJ0-2Mix dataset. To assess our model in more realistic conditions, we also considered the WHAM! [29] dataset, which contains mixtures corrupted by non-stationary environmental noise. In addition to the non-causal offline scenario we provide experimental evidence in a real-time low-latency scenario by considering causal versions of the RE-SepFormer. In detail, our contributions are the following:

- We show that the RE-SepFormer reaches a competitive performance on the popular WSJ0-2Mix and WHAM! datasets in both causal and non-causal settings.
- With the RE-SepFormer, we achieve a 3x reduction of the parameters and 11x reduction of the multiply-accumulate operations (MACs) per second over the standard SepFormer.
- The RE-SepFormer is extremely parallelizable, and therefore highly suitable for GPU inference. It scales significantly better than the previous Transformer-based architectures in terms of memory and inference time, making it more suitable for processing long mixtures.

2. RE-SEPFORMER

2.1. Time-Domain Masking Architecture

The overall architecture of the RE-SepFormer is shown in Fig. 1. Similar to other popular architectures such as Conv-TasNet [15], Dual-Path RNN [16], and SepFormer [30], our model is based on learned-domain masking. The input mixture $x \in \mathbb{R}^T$ is first passed through an encoder, which outputs a latent representation $h \in \mathbb{R}^{T' \times F}$ using a strided convolutional layer:

$$h = \text{ReLU}(\text{conv1d}(x)). \quad (1)$$

The masking network takes in the representation h , and produces the masks $m_1, m_2 \in \mathbb{R}^{T' \times F}$. We consider here a model with two

^{*}Equal contribution.

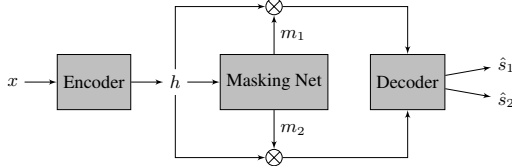


Fig. 1: An high-level description of the masking-based source separation pipeline: the encoder learns a latent representation h from the input mixture x . The masking network then estimates the optimal masks m_1 and m_2 to separate the sources in the mixture. Finally, the decoder reconstructs the sources from the masked representations.

sources without loss of generality. The decoder is a transposed convolutional layer that reconstructs the time-domain signals \hat{s}_1 and \hat{s}_2 from the masked latent representations:

$$\hat{s}_k = \text{conv1d-transpose}(m_k * h). \quad (2)$$

2.2. The Masking Network

The architecture of the masking network is depicted in Fig. 2 (top). Firstly, the input representation is split into temporal chunks. We denote this tensor with $h' \in \mathbb{R}^{C \times N_c \times F}$, where C is the size of each chunk, and N_c is the resulting number of chunks. As opposed to the standard SepFormer, we use non-overlapping chunks to reduce the amount of computations. Then, the RE-SepFormer processes the chunks h' and provides a latent representation $h'' \in \mathbb{R}^{C \times N_c \times N_s \times F}$ (where N_s denotes the number of sources). The tensor h'' is further transformed by a PReLU activation function and a linear layer. Finally, the chunking is undone by simply concatenating the chunks on the original time axis. We denote the resulting tensor with $h''' \in \mathbb{R}^{T' \times N_s \times F}$. The final masks are estimated by passing this tensor through a ReLU non-linearity.

2.3. Resource Efficient SepFormer

The RE-SepFormer block is detailed in Fig. 2 (bottom). This module includes three main components: the *IntraTransformer1*, the *MemoryTransformer*, and the *IntraTransformer2*. The *IntraTransformer1* is applied to the time axis of all of the chunks and generates a tensor $e_1 \in \mathbb{R}^{C \times N_c \times F}$. The goal of this block is to process short-term temporal information. We then compute a summary representation $e_2 \in \mathbb{R}^{N_c \times F}$ by averaging this tensor over the time axis. The intuition behind this operation is that the average over the time-axis of a latent representation can provide enough high-level contextual information to embed longer-term dependencies. Working with a summary vector is much more computationally convenient than operating on the full tensor e_1 as done in the original SepFormer. This saves significant amounts of computations.

This summary representation e_2 is then fed into the Memory Transformer. The latter is applied to the chunk axis and produces a representation $e_3 \in \mathbb{R}^{N_c \times F}$ that models long-term dependencies across chunks. The e_3 tensor is then added element-wise to e_1 (with broadcasting over the time axis). The resulting e_4 tensor is particularly rich as it incorporates both short and long-term dependencies. Note also that this operation implicitly adds a gradient shortcut in the architecture, contributing to making the architecture easier to train and more robust against vanishing gradient issues.

Finally, we provide more capacity to the model by feeding e_4 into another *IntraTransformer2* operating on the time axis. This generates the tensor $h'' \in \mathbb{R}^{C \times N_c \times N_s \times F}$, that is the output of the RE-SepFormer block.

3. EXPERIMENTAL SETUP

3.1. Datasets

We provide experimental evidence on the popular WSJ0-2Mix dataset [31], which is a standard benchmark largely adopted in speech separation. The training, validation, and test partitions consist of 30, 10, and 5 hours of speech. The mixtures are created by randomly mixing utterances using random relative gains between 0 dB and 5 dB. In the training and test sets, different speakers are used. We also assess our models on the WHAM! corpus [29], which adds non-stationary noises such as background noise from restaurants, bars, and parks with different SNRs to the mixtures.

3.2. Models

We compare the RE-SepFormer against popular speech separation methods (e.g., TasNet, Conv-TasNet, Dual-Path RNN, etc.). Moreover, we compare our model with SkiM [19], which is an RNN-based model recently proposed to perform computationally-efficient speech separation. We obtained the implementation of SkiM [19] from the ESPnet toolkit [32] and used the default parameter setting reported in the original paper. We also compare against SepFormer-Light that has 6.4M parameters down from 25.7M. For this reduction, we used 128 encoder outputs and 512 dimensions in the feed-forward layers of the Transformer. The implementation of RE-SepFormer is available in the SpeechBrain [33] GitHub repository¹.

We consider both the causal and non-causal versions of these models. The causal version of the RE-SepFormer uses triangular matrices in the attention mechanisms that prevent attending to future time steps. For the RE-SepFormer, we used 128 convolutional filters in the convolutional encoder. We used 8 Transformer layers for the Intra and Memory Transformers with 8 parallel attention heads and 1024 dimensional positional feed-forward layers. The chunk size is set to 150 samples.

3.3. Training Details

The model is trained with the permutation invariant SI-SNR loss [15, 34, 35] and the parameters are updated with the Adam optimizer [36]. We halve the learning rate after epoch 85 if the performance on the validation set does not improve for 3 consecutive epochs. We train the model with dynamic mixing (DM) [37, 38], which generates new mixtures on-the-fly by randomly mixing clean utterances. For more details, please refer to the reference WSJ0-Mix recipe available on SpeechBrain [33].

4. RESULTS

4.1. From SepFormer to RE-SepFormer

In Table 1 we show the impact of the architectural changes done to derive the RE-SepFormer from the original SepFormer in terms of performance, number of parameters, and MACs using the standard WSJ0-2Mix dataset (non-causal setting).

The first modification is the use of non-overlapped chunks. From Table 1, it emerges that there is a significant performance drop when we adopt this change (see first two lines). The SDRi, for instance, drops from 22.4 dB (standard SepFormer) to 16.2 dB. On the other hand, we significantly reduce the MACs by 2.5x.

¹<https://github.com/speechbrain/speechbrain/tree/develop/recipes/WSJ0Mix/separation>

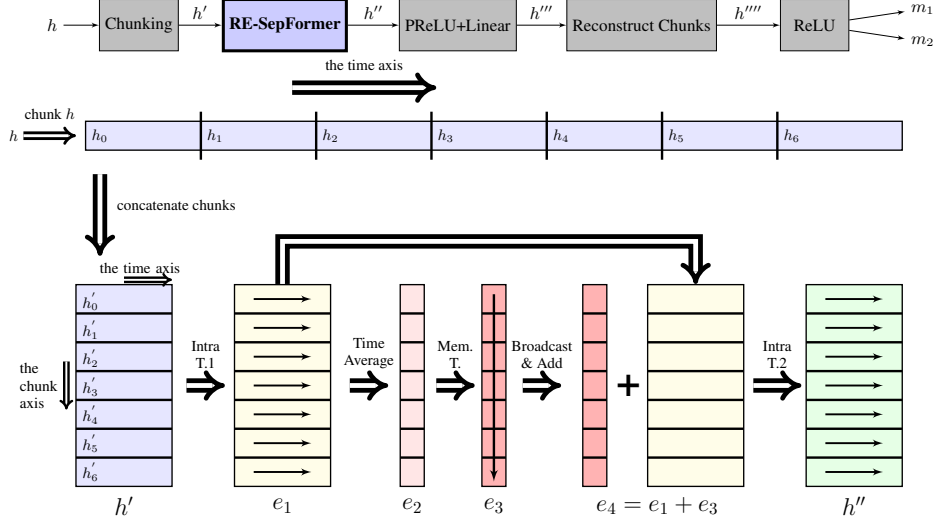


Fig. 2: (Top) The architecture of the masking network. **(Bottom)** The Resource-Efficient SepFormer module: (1) the latent representation h is chunked to get $h'_0, h'_1, \dots, h'_{N_c}$ (2) the IntraTransformer is applied to all of the chunks independently (3) the output is averaged over the time dimension and passed through the memory Transformer (4) the resulting vector is added to the output of the IntraTransformer with broadcasting over the time axis (5) the resulting tensor is passed through another IntraTransformer to obtain the final output h'' .

Table 1: Comparison of SepFormer and RE-SepFormer on WSJ0-2Mix, non-causal setting.

Model	Overlap	Avg	SI-SNRi (dB)	SDRI (dB)	#Params (M)	GMACs/s
SepFormer	50%	×	22.3	22.4	25.7	69.6
SepFormer	0%	×	15.9	16.2	25.7	28.0
RE-SepFormer	0%	✓	18.6	18.9	8.0	6.3

The other proposed intervention is the summary representation (time average) processed by a Memory Transformer. This operation drastically reduces the number of parameters (3.2x reduction) and the MACs (11x reduction). Interestingly, this modification not only does not deteriorate the separation performance but even yields a slight improvement, possibly due to the fact that the averaging operation better promotes continuity between the latent chunks. We believe that the RE-SepFormer is particularly interesting for small-footprint devices. Even though the performance drop is not negligible compared to the standard SepFormer, the model still provides very high-quality speech separation (SDRI up to 18.9 dB) with a drastic reduction of computational resources.

4.2. Comparison with SkiM

Table 2 compares the performance of the RE-SepFormer with SkiM [19] on WSJ0-2Mix and WHAM! in causal and non-causal settings. SkiM [19] is a recently proposed model for efficient speech separation. It uses RNNs with non-overlapping chunks, making it a natural benchmark. For a fair comparison, we use dynamic mixing and the same kernel size in the convolutional layers ($kernel_{size} = 16$) for both models.

As shown in Table 2, the RE-SepFormer outperforms SkiM in three of the four tested conditions: it provides better performance on the WSJ0-2Mix dataset (both causal and non-causal settings) and on the WHAM! corpus (causal setting). SkiM, on the other hand, slightly outperforms the RE-SepFormer in the non-causal modality only. SkiM also uses fewer MACs/s than the RE-SepFormer (3.7G versus 6.3G). However, as we will show in the next section, this has no impact on latency. Remarkably, even when handling long sequences, RE-SepFormer matches SkiM in terms of memory usage and inference speed.

Table 2: Comparison of RE-SepFormer and SkiM on WSJ0-2Mix and WHAM!.

Model	Dataset	Causal		Non-Causal	
		SI-SNRi (dB)	SDRI (dB)	SI-SNRi (dB)	SDRI (dB)
SkiM	WSJ0-2Mix	13.2	13.5	18.1	18.3
RE-SepFormer	WSJ0-2Mix	14.2	14.5	18.6	18.9
SkiM	WHAM!	10.6	11.0	14.5	14.8
RE-SepFormer	WHAM!	11.3	11.7	14.1	14.4

4.3. Speed and Memory Utilization

In Fig. 3, we compare the memory usage (left) and the inference time (right) of the RE-SepFormer, SkiM, and SepFormer. For a more meaningful comparison, we use a SepFormer (denoted as SepFormer-Light) with a reduced number of parameters (i.e., 6.4 M). This experiment has been conducted on an NVIDIA A100 GPU considering different input lengths (ranging from 1 to 256 seconds).

The RE-SepFormer turned out to scale significantly better than the SepFormer-Light due to the summary representation. The most impressive result is the inference time observed when feeding the RE-SepFormer with long sequences. For an input of 256 seconds, the RE-SepFormer is 7x faster than SepFormer-Light. Furthermore, it results in a memory usage reduction of up to 28% for long sequences.

It is worth noting that the RE-SepFormer is composed of self-attention blocks that consist of feed-forward layers. This feature makes the overall architecture highly parallelizable. In contrast, SkiM is mainly composed of RNN (LSTM) layers, which require sequential processing. This potentially explains why it is not faster than RE-SepFormer, despite using only 60% of the MACs.

4.4. Comparison with Other Models

In Table 3, we compare the performance of RE-SepFormer with a wide range of models from the literature (WSJ0-2Mix, non-causal setting). Despite its efficiency, we observe that RE-SepFormer achieves competitive performance. For example, RE-SepFormer performs comparably to Dual-Path RNN, while being significantly more efficient in terms of MACs. The RE-SepFormer outperforms the popular Conv-TasNet, and SuDoRM-RF models. We also compare against

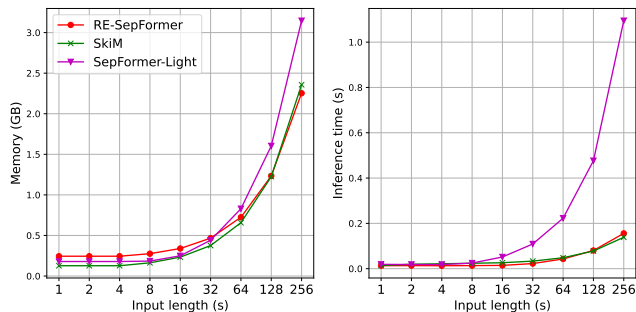


Fig. 3: Memory in GB (left panel) and inference time in seconds (right panel) comparison of RE-SepFormer, SkiM and SepFormer-Light. The x-axis in both panels shows the length of the input signal in seconds (8 kHz sampling rate).

popular efficient Transformer architectures (i.e., Reformer and Longformer) applied without chunking [18]. The RE-SepFormer outperforms aforementioned efficient Transformers as well.

4.5. Ablation Studies

To assess the relative importance of each component to the overall performance, we conduct the following ablation studies: (1) we decrease to 4 the number of layers in the IntraTransformer and Memory Transformer modules; (2) we reduce to 512 the dimension of the positional feed-forward layers in the IntraTransformer and Memory Transformer modules; (3) we combine all the previous ablations.

Table 4 shows the results. Modifications to the IntraTransformers lead to the most significant performance drop together with the most substantial reduction in the number of parameters and MACs. In particular, halving the number of layers has the largest impact. On the contrary, when we perform ablations on the Memory Transformer, we observe minimal effects on both the performance and MACs, despite a moderate reduction in the number of parameters.

It is worth noting that when we combine all the ablations, we still achieve an acceptable SDRi, surpassing methods like TasNet, SignPredictionNet and Conv-TasNet, while utilizing significantly fewer parameters and MACs. This further highlights the suitability of RE-SepFormer for small-footprint devices.

5. CONCLUSIONS

In this paper, we proposed the RE-SepFormer, which is a contribution towards more efficient speech separation with Transformers. The RE-SepFormer uses non-overlapping blocks and relies on compact latent summaries calculated from each chunk rather than attending all the time steps. Our experiments, conducted on the WSJ0-2Mix and WHAM! datasets in both causal and non-causal settings, show that the RE-SepFormer achieves an SDRi of 18.9 dB on WSJ0-2Mix and 14.4 dB on WHAM!. Compared to the SepFormer, it employs more than 3x fewer parameters with a 11x reduction of the MACs. The model is mainly composed of feed-forward layers, and it is thus highly parallelizable. As a result, it scales significantly better than the previous Transformer-based architectures in terms of memory and inference time, making it more suitable for processing long mixtures. This feature makes the RE-SepFormer particularly suitable for real-time low-latency speech separation on small-footprint devices such as GPU-equipped smartphones or laptops.

Table 3: Best results on the WSJ0-2Mix dataset (test-set) for non-causal models.

Model	SI-SNRi (dB)	SDRi (dB)	#Params (M)	GMACs/s
TasNet [39]	10.8	11.1	-	-
SignPredictionNet [40]	15.3	15.6	55.2	-
Conv-TasNet [15]	15.3	15.6	5.1	3.2 [19]
Two-Step CTN [37]	16.1	-	8.6	-
MGST [41]	17.0	17.3	-	-
DeepCASA [42]	17.7	18.0	12.8	-
FurcaNeXt [43]	-	18.4	51.4	-
Dual-Path RNN [16]	18.8	19.0	2.6	38.9 [19]
SuDoRM-RF [17]	17.0	-	2.6	-
DPTNet [44]	20.2	20.6	2.6	-
SkiM [19] + DM	18.2	18.4	14.5	3.7
SepFormer [30] + DM	22.3	22.4	25.7	69.6
SepFormer Light + DM	20.0	20.2	6.4	17.5
Reformer [18] + DM	16.7	16.9	12.0	12.4
Longformer [18] + DM	13.1	13.4	15.1	12.3
SepIt + DM [45]	22.4	-	4.6	-
TFPSNet [46]	21.1	21.3	2.7	29.6 [47]
TF-GridNet [47]	-	23.6	14.5	231.1 [47]
MossFormer + DM [48]	22.8	-	42.1	42.7
RE-SepFormer + DM	18.6	18.9	8.0	6.3

Table 4: Ablation studies on the number of intra/memory layers and the intra/memory positional feed-forward layer dimension (d_{ff}), non-causal setting.

#Intra	Intra d_{ff}	#Memory	Memory d_{ff}	SDRi (dB)	#Params (M)	GMACs/s
8	1024	8	1024	18.9	8.0	6.3
4	1024	8	1024	16.4	5.3	3.2
8	512	8	1024	18.3	5.8	4.0
8	1024	4	1024	18.5	6.6	6.2
8	1024	8	512	18.7	6.9	6.2
4	512	4	512	16.5	2.4	2.0

6. REFERENCES

- [1] T. Brown et al., “Language models are few-shot learners,” in *NeurIPS*, 2020, pp. 1877–1901.
- [2] A. Chowdhery et al., “PaLM: Scaling language modeling with pathways,” *arXiv preprint arXiv:2204.02311*, 2022.
- [3] M. Shoyebi, M. Patwary, R. Puri, P. LeGresley, J. Casper, and B. Catanzaro, “Megatron-LM: Training multi-billion parameter language models using model parallelism,” *arXiv preprint arXiv:1909.08053*, 2020.
- [4] A. Baevski, Y. Zhou, A. Mohamed, and M. Auli, “wav2vec 2.0: A framework for self-supervised learning of speech representations,” in *NeurIPS*, 2020, pp. 12449–12460.
- [5] W.-N. Hsu et al., “HuBERT: Self-supervised speech representation learning by masked prediction of hidden units,” *IEEE/ACM Trans. Audio, Speech and Lang. Proc.*, pp. 3451–3460, 2021.
- [6] T. Parcollet and M. Ravanelli, “The energy and carbon footprint of training end-to-end speech recognizers,” in *Interspeech*, 2021.
- [7] N. Tomashenko et al., “Introducing the voiceprivacy initiative,” in *Interspeech*, 2020.
- [8] G. Hinton, O. Vinyals, and J. Dean, “Distilling the knowledge in a neural network,” in *NeurIPS Deep Learning and Representation Learning Workshop*, 2015.
- [9] R. Reed, “Pruning algorithms—a survey,” *IEEE Transactions on Neural Networks*, pp. 740–747, 1993.
- [10] P. Molchanov, S. Tyree, T. Karras, T. Aila, and J. Kautz, “Pruning convolutional neural networks for resource efficient inference,” in *ICLR*, 2017.

- [11] M. Kim and P. Smaragdis, “Bitwise neural networks for efficient single-channel source separation,” in *ICASSP*, 2018, pp. 701–705.
- [12] I. Hubara, M. Courbariaux, D. Soudry, R. El-Yaniv, and Y. Bengio, “Quantized neural networks: Training neural networks with low precision weights and activations,” *JMLR*, 2017.
- [13] D. Yin, C. Luo, Z. Xiong, and W. Zeng, “PHASEN: A phase-and-harmonics-aware speech enhancement network,” in *AAAI*, 2020.
- [14] Y. Hu et al., “DCCRN: Deep complex convolution recurrent network for phase-aware speech enhancement,” in *Interspeech*, 2020.
- [15] Y. Luo and N. Mesgarani, “Conv-TasNet: Surpassing ideal time–frequency magnitude masking for speech separation,” *IEEE/ACM Trans. Audio, Speech and Lang. Proc.*, pp. 1256–1266, 2019.
- [16] Y. Luo, Z. Chen, and T. Yoshioka, “Dual-path RNN: efficient long sequence modeling for time-domain single-channel speech separation,” in *ICASSP*, 2020, pp. 46–50.
- [17] E. Tzinis, Z. Wang, and P. Smaragdis, “SuDoRM-RF: Efficient networks for universal audio source separation,” in *MLSP*, 2020, pp. 1–6.
- [18] C. Subakan, M. Ravanelli, S. Cornell, F. Grondin, and M. Bronzi, “Exploring self-attention mechanisms for speech separation,” *IEEE/ACM Trans. Audio, Speech and Lang. Proc.*, pp. 2169–2180, 2023.
- [19] C. Li, L. Yang, W. Wang, and Y. Qian, “SkiM: Skipping memory LSTM for low-latency real-time continuous speech separation,” in *ICASSP*, 2022.
- [20] H. Mazzawi et al., “Improving keyword spotting and language identification via neural architecture search at scale,” in *Interspeech*, 2019, pp. 1278–1282.
- [21] X. Wu, S. Hu, Z. Wu, X. Liu, and H. Meng, “Neural architecture search for speech emotion recognition,” in *ICASSP*, 2022, pp. 6902–6906.
- [22] S. Hu et al., “Neural architecture search for LF-MMI trained time delay neural networks,” in *ICASSP*, 2021, pp. 6758–6762.
- [23] A. Vaswani et al., “Attention is all you need,” in *NeurIPS*, 2017.
- [24] Y. Tay, M. Dehghani, D. Bahri, and D. Metzler, “Efficient transformers: A survey,” *ACM Comput. Surv.*, 2022.
- [25] S. Wang, B. Z. Li, M. Khabisa, H. Fang, and H. Ma, “Linformer: Self-attention with linear complexity,” *arXiv preprint arXiv:2006.04768*, 2020.
- [26] I. Beltagy, M. E. Peters, and A. Cohan, “Longformer: The long-document transformer,” *arXiv preprint arXiv:2004.05150*, 2020.
- [27] N. Kitaev, L. Kaiser, and A. Levskaya, “Reformer: The efficient transformer,” in *ICLR*, 2020.
- [28] S. Kim et al., “Squeezeformer: An efficient transformer for automatic speech recognition,” in *NeurIPS*, 2022, pp. 9361–9373.
- [29] G. Wichern et al., “WHAM!: Extending speech separation to noisy environments,” in *Interspeech*, 2019.
- [30] C. Subakan, M. Ravanelli, S. Cornell, M. Bronzi, and J. Zhong, “Attention is all you need in speech separation,” in *ICASSP*, 2021.
- [31] J. Hershey, Z. Chen, J. Le Roux, and S. Watanabe, “Deep clustering: Discriminative embeddings for segmentation and separation,” in *ICASSP*, 2016, pp. 31–35.
- [32] H. Inaguma et al., “ESPnet-ST: All-in-one speech translation toolkit,” in *ACL: System Demonstrations*, 2020, pp. 302–311.
- [33] M. Ravanelli et al., “SpeechBrain: A general-purpose speech toolkit,” *arXiv preprint arXiv:2106.04624*, 2021.
- [34] M. Kolbæk, D. Yu, Z.-H. Tan, and J. Jensen, “Multitalker speech separation with utterance-level permutation invariant training of deep recurrent neural networks,” *IEEE/ACM Trans. Audio, Speech and Lang. Proc.*, pp. 1901–1913, 2017.
- [35] J. Le Roux, S. Wisdom, H. Erdogan, and J. R. Hershey, “SDR–half-baked or well done?,” in *ICASSP*, 2019, pp. 626–630.
- [36] D. P. Kingma and J. Ba, “Adam: A method for stochastic optimization,” 2015, ICLR.
- [37] E. Tzinis, S. Venkataramani, Z. Wang, C. Subakan, and P. Smaragdis, “Two-step sound source separation: Training on learned latent targets,” in *ICASSP*, 2020, pp. 31–35.
- [38] N. Zeghidour and D. Grangier, “Wavesplit: End-to-end speech separation by speaker clustering,” *IEEE/ACM Trans. Audio, Speech and Lang. Proc.*, pp. 2840–2849, 2021.
- [39] Y. Luo and N. Mesgarani, “TasNet: time-domain audio separation network for real-time, single-channel speech separation,” in *ICASSP*, 2018, pp. 696–700.
- [40] Z.-Q. Wang, K. Tan, and D. Wang, “Deep learning based phase reconstruction for speaker separation: A trigonometric perspective,” in *ICASSP*, 2019, pp. 71–75.
- [41] Y. Zhao, C. Luo, Z.-J. Zha, and W. Zeng, “Multi-scale group transformer for long sequence modeling in speech separation,” in *IJCAI*, 2020, pp. 3251–3257.
- [42] Y. Liu and D. Wang, “Divide and conquer: A deep CASA approach to talker-independent monaural speaker separation,” *IEEE/ACM Trans. Audio, Speech and Lang. Proc.*, 2019.
- [43] Z. Shi, H. Lin, L. Liu, R. Liu, J. Han, and A. Shi, “FurcaNeXt: End-to-end monaural speech separation with dynamic gated dilated temporal convolutional networks,” in *MultiMedia Modeling*, 2020, pp. 653–665.
- [44] J. Chen, Q. Mao, and D. Liu, “Dual-path transformer network: Direct context-aware modeling for end-to-end monaural speech separation,” in *Interspeech*, 2020, pp. 2642–2646.
- [45] S. Lutati, E. Nachmani, and L. Wolf, “SepIt: Approaching a single channel speech separation bound,” in *Interspeech*, 2022, pp. 5323–5327.
- [46] L. Yang, W. Liu, and W. Wang, “TFPSNet: Time-frequency domain path scanning network for speech separation,” in *ICASSP*, 2022, pp. 6842–6846.
- [47] Z.-Q. Wang, S. Cornell, S. Choi, Y. Lee, B.-Y. Kim, and S. Watanabe, “TF-GridNet: Integrating full- and sub-band modeling for speech separation,” *IEEE/ACM Trans. Audio, Speech and Lang. Proc.*, pp. 3221–3236, 2023.
- [48] S. Zhao and B. Ma, “MossFormer: Pushing the performance limit of monaural speech separation using gated single-head transformer with convolution-augmented joint self-attentions,” in *ICASSP*, 2023.